

¹Ms. Seema B.
Rathod

²Dr. Lata L. Ragha

DLCT LUNG Detect Net: Leveraging Deep Learning for Lung Tumor Detection in CT scans



Abstract: - Lung cancer is a critical global health concern, necessitating precise early diagnosis and intervention for better patient outcomes. Computed Tomography (CT) scans are pivotal in lung cancer detection, and leveraging advanced technology is crucial. This study introduces "DLCTLungDetectNet," a Convolutional Neural Network (CNN) based deep learning framework, with a focus on early lung cancer detection using CT scan images. The core innovation lies in the integration of the robust "FusionNet," a hybrid model amalgamating feature from ResNet50 and InceptionV3. We conduct a comprehensive comparative analysis, showcasing the superior performance of DLCTLungDetectNet over established architectures such as VGG16, VGG19, and Inception v3. Rigorous evaluation based on standard metrics substantiates DLCTLungDetectNet's high accuracy, precision, Area Under Curve (AUC), and F1 score. This research not only highlights the potential of deep learning in enhancing lung cancer diagnosis but also establishes a benchmark, showcasing the efficacy of the FusionNet hybrid model for achieving superior accuracy in automated lung tumor detection.

Keywords: Lung cancer, CT scan imaging, Deep Learning, CNN, FusionNet, VGG16, VGG19, Inception v3, ResNet50.

I. INTRODUCTION

Lung cancer remains one of the most formidable and prevalent health challenges globally, significantly impacting public health and necessitating urgent, accurate diagnoses for effective treatment and improved patient outcomes. Early detection and timely intervention are paramount in mitigating the mortality rates associated with lung cancer. In the realm of medical imaging, Computed Tomography (CT) scans have emerged as indispensable tools for lung cancer detection, offering high-resolution images that are crucial for precise diagnosis. The intricate and nuanced patterns present in these images, however, demand sophisticated analytical approaches for accurate interpretation. In recent years, the integration of deep learning methodologies, particularly Convolutional Neural Networks (CNNs), has shown remarkable promise in automating the analysis of medical images and aiding healthcare professionals in accurate diagnostics. Deep Learning for Lung Tumor Detection in CT scans (DLCTLungDetectNet) presents a concerted effort to harness the potential of CNN-based deep learning frameworks specifically designed for early lung cancer detection using CT scan images. This study explores an innovative approach to feature extraction and classification, aiming to significantly enhance the accuracy and efficiency of lung tumor detection compared to traditional methods. DLCTLungDetectNet's strength lies in its unique hybrid model, FusionNet, which expertly merges features extracted from ResNet50 and InceptionV3. This fusion of influential pre-trained models enhances the network's ability to capture intricate patterns and complex features within the lung images, ultimately bolstering the accuracy of tumor detection. The proposed framework undergoes thorough evaluation and comparison with other prominent deep learning architectures, namely VGG16, VGG19, and Inception v3, to validate its superior performance in terms of accuracy, precision, Area Under Curve (AUC), and F1 score.

This research not only underscores the potential of deep learning in revolutionizing lung cancer diagnostics but also emphasizes the significance of model fusion strategies for achieving superior accuracy in automated lung tumor detection. The subsequent sections delve into the methodology, dataset specifics, proposed CNN architecture, results, and discussions, providing comprehensive insights into DLCTLungDetectNet and its pivotal role in advancing the field of lung cancer detection using CT scan imaging.

¹ Research Scholar Lokmanya Tilak College of Engineering

Navi Mumbai University, India

omseemarathod@gmail.com

²Fr. C. Rodrigues Institute of Technology

Navi Mumbai University, India

lata.ragha@fcrit.ac.in

II. RELATED WORK

Traditional image processing techniques are employed to enhance image quality in this research [2] To ensure accurate diagnoses, improving the quality of medical images is essential. This research employs the highly effective Discrete Wavelet Transform method for noise removal in the images. [3] In this research, the authors used the Wiener and median filters in pre-processing. The filters were compared using the PSNR parameter, and the results demonstrated that the Wiener filter outperformed the median filter, yielding superior results [4]. In this research, the median, bilateral, and discrete cosine transformation techniques were used to remove noise from images. EEG data was utilized as input for the study. [5] The objective of this study is to generate high-quality images using nonlinear filtering algorithms. Evaluation is based on parameters such as PSNR, MSE, SNR, and MAE. [6] In all the research, various filters are employed for pre-processing and improving the image quality. These include Wavelet Transform, NL-means filters, multiple filters such as average, Gaussian, log, median, and Wiener filters, as well as the Gaussian filter. [7,8,9,10]. Implemented in this method are image processing and machine learning approaches for predicting and distinguishing between tumour and non-tumour forms based on CT scan images. Evaluation parameters include geometrical, statistical, and gray-level characteristics. The system achieves an accuracy of 84%, sensitivity of 97.14%, and specificity of 53.33%. Nevertheless, the accuracy of tumour detection is deemed unsatisfactory, and the absence of machine learning methods underscores the necessity for a new model capable of offering enhancements and probabilistic information. [11,12]. The CAD system utilizes the CNN algorithm for classification, achieving an accuracy of 84.6%, sensitivity of 82.5%, and specificity of 86.7%. However, the training phase reduces time but does not yield satisfactory accuracy. [13] The model incorporates the k-means algorithm for segmentation. Images are converted into GLCM form, and parameters like entropy, correlation, homogeneity, PSNR, and SSIM are used for result analysis. An accuracy of 90.7% is achieved, but further improvements are required to enhance accuracy. [14] The model utilizes fuzzy inference methods for lung tumour detection. The system employs grey transformation to improve image quality. Features such as area, mean, entropy, and correlation are extracted and used to train a classification model. [15]. The model incorporates watershed segmentation and Gabor filter for pre-processing. Accuracy is compared with a neural fuzzy base. Achieved accuracy is 90.1%, but it does not provide classification into benign or malignant categories. [16,17]. The model utilizes SVM algorithm for classification. The system uses CT scan images along with priori information and Hounsfield Unit values to calculate the region of interest. [18,19].

The cited papers encompass a broad spectrum of methodologies and applications within medical imaging, particularly in the realm of detecting, identifying, and classifying lung diseases, with a specific focus on lung cancer and pulmonary nodules. Each study employs unique techniques, datasets, and deep learning architectures tailored to tackle specific challenges in this domain. For instance, [21] utilizes a level-set approach to perform joint image segmentation and registration in CT lung images, offering an integrated framework for these tasks. However, its applicability is confined to CT lung imaging, limiting its usage in other modalities or anatomical regions. [22] employs Dense Convolutional Binary-Tree Networks to identify lung nodules, but its effectiveness is impeded by the scarcity of large training datasets, potentially compromising its generalization capabilities. Similarly, [23] uses deep learning for identifying and classifying lung nodules, demonstrating potential in enhancing radiologist performance. Nonetheless, it is constrained by dataset availability and dependencies on image quality. In [24], a Deep 3D Residual CNN is deployed to minimize false-positive identifications of lung nodules while maintaining high accuracy. Nonetheless, its performance may fluctuate depending on input image quality.[25] utilizes Deep Convolutional Neural Networks across diverse datasets, but its efficacy relies on the availability of massive data and may struggle with poor-quality images.Both [26] and [36] concentrate on predicting EGFR mutation in lung adenocarcinoma using deep learning, although they face limitations due to small dataset sizes.[27] and [29] emphasize reducing false positives and improving precision in lung cancer identification, respectively. However, they require large datasets and specialized knowledge.[30] addresses inter-observer variability in diagnosing lung nodules but depends on large datasets and specialized knowledge.[31] underscores high efficiency in lung cancer screening, while [32] focuses on accurately determining the stage of lung cancer, both grappling with challenges related to image quality dependency.[33] and [34] adopt CNN-based approaches for nodule detection and classification, enhancing efficiency but facing constraints due to dataset sizes.[35] emphasizes accurate categorization of lung images, [37] focuses on early detection of pulmonary nodules, [38] on non-intrusive lung cancer prediction, and [39] on improved prognosis, all requiring large datasets and specialized knowledge.[40] and [41] highlight high accuracy in nodule classification and cancer prediction but are hindered by small dataset sizes.[42] and [44] concentrate on precision in evaluating PD-L1 expression and cardiovascular disease risk

assessment, respectively, necessitating large datasets and computational power.[43] and [45] stress automated extraction and invasive-free detection of lung cancer, respectively, yet are confined by specific dataset requirements.[46] enhances diagnostic precision in non-small cell lung cancer detection, albeit constrained by dataset size requirements.[47] proposes early detection of lung nodules using machine learning, [48] improves access to lung cancer screening, and [49] enhances accuracy in nodule detection, all encountering challenges related to sample sizes.Lastly, [50] and [51] introduce novel approaches for cancer prediction and detection, respectively, while [52] focuses on reducing false positives in detection tasks, each grappling with specific limitations such as the absence of integration with optimization techniques or restricted dataset usage.

III. METHODOLOGY

we initiated by gathering a publicly available Lung Cancer dataset, specifically utilizing the Kaggle dataset, which encompasses 1080 CT scan images. Upon dataset collection, we applied preprocessing techniques aimed at enhancing image quality, extracting pertinent features, and ultimately aiding radiologists and healthcare professionals in achieving precise diagnoses. Post-preprocessing, we applied various Deep Learning Frameworks, including VGG16, VGG19, Inception v3, and ResNet50, Fusion Net, to the computerized tomography (CT) scan dataset, using the standard hold-out-validation technique for comparison, alongside our proposed design. Out of the complete dataset, 70% was assigned for training, 20% for testing, and 10% for validation. Subsequently, we classified the CT scan images into categories: normal, benign, and malignant. We then conducted a thorough result analysis for each deep learning model and our proposed model to derive insightful conclusions.

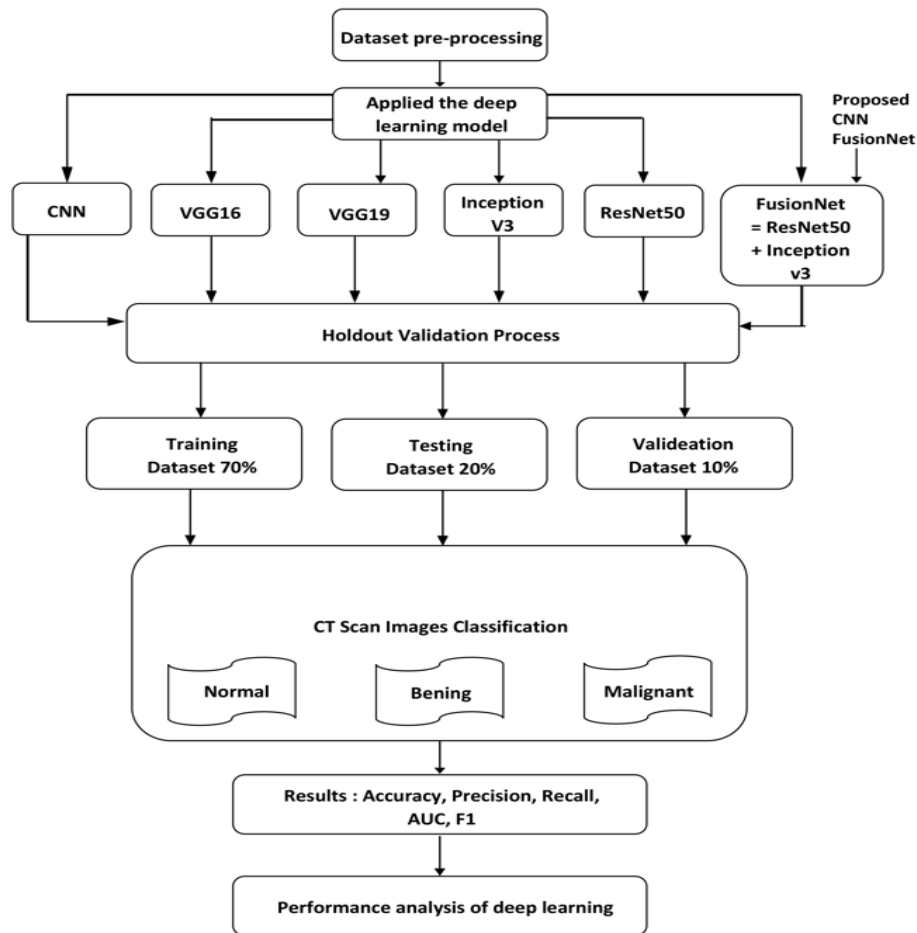


Figure. 1 depicts an overview of the proposed strategy

➤ **Main Objective and Novelty:**

The primary objectives of "DLCTLungDetectNet: Deep Learning for Lung Tumor Detection in CT Scans" can be succinctly outlined as follows:

- Lung Tumor Detection: Develop DLCTLungDetectNet, a specialized deep learning model, to accurately detect lung tumors in CT scans.
- Enhanced Accuracy and Reliability: Improve detection accuracy and reliability compared to traditional methods, focusing on minimizing false positives and false negatives.
- Early-Stage Diagnosis: Enable early diagnosis of lung tumors through automated analysis of medical images, potentially leading to improved patient outcomes by detecting tumors at initial stages.
- Operational Efficiency: Streamline the tumor detection process by automating analysis, reducing the workload on radiologists, and expediting the diagnostic procedure.
- Clinical Viability: Ensure DLCTLungDetectNet's practicality and clinical relevance for healthcare professionals, bolstering the domain of medical imaging and lung cancer diagnosis.
- Adaptability and Scalability: Design the deep learning model to be adaptable and scalable for potential integration into broader healthcare systems and facilities.
- Contribution to Medical AI: Contribute to the evolving field of deep learning applications in medical imaging by providing a specialized solution for lung tumor detection.
- Enhanced Patient Care: Ultimately, strive to enhance patient care and outcomes by facilitating earlier and more accurate detection of lung tumors through advanced AI techniques.

IV. DATASET COLLECTION

In our research project, we focused on the detection of chest cancer utilizing advanced artificial intelligence framework, including machine learning and convolutional neural networks (CNN). Our objective was to classify and diagnose patients for the presence of cancer and provide essential information about the specific type of cancer along with recommended treatment options.

Dataset Details:

Our dataset was meticulously curated from various sources to ensure the availability of comprehensive and diverse data for training and evaluation of our AI model. The data primarily comprises medical images in JPG and PNG formats to facilitate compatibility with our CNN architecture. The dataset encompasses three distinct types of chest cancers and a category for normal chest scans. Below is a breakdown of the dataset structure:

Main Folder (Data): This is the root directory containing subfolders for different dataset splits.

Subfolders:

- a) Training Set (Train): This set comprises 70% of the data and serves as the primary dataset for training our AI model.
- b) Testing Set (Test): Containing 20% of the data, this set is reserved for evaluating the model's performance.
- c) Validation Set (Valid): With 10% of the data, this set ensures robust validation during model development and tuning.

Cancer Types:

Our dataset features three prominent chest cancer types:

- i. Adenocarcinoma: Lung adenocarcinoma, the most common subtype of lung cancer, represents around 30% of all lung cancer cases and approximately 40% of non-small cell lung cancer diagnoses. Typically, these tumors are located in the lung's peripheral areas, primarily within the glands responsible for mucus production. Indications of this condition may manifest as coughing, hoarseness, unexplained weight loss, and a sense of weakness
- ii. Large Cell Carcinoma: Large-cell undifferentiated carcinoma is recognized for its rapid growth and extensive spread throughout the lung. It typically constitutes 10-15% of all instances of non-small cell lung cancer and is renowned for its highly aggressive behavior.

- iii. Squamous Cell Carcinoma: Squamous cell lung cancer is primarily situated in the central regions of the lung, often at the convergence of the larger bronchi with the trachea or within significant airway branches. It constitutes approximately 30% of non-small cell lung cancers and exhibits a strong association with smoking.
- iv. Normal Chest Scans: In addition to cancerous samples, our dataset includes a category of normal chest CT-scan images for comparative analysis.

This well-structured dataset served as the foundation for our machine learning and CNN framework, enabling us to develop a robust and accurate chest cancer detection system.

4.1 Data Pre-processing

Image processing techniques play a crucial role in lung cancer detection from medical images like X-rays and CT scans. These techniques help in enhancing image quality, extracting relevant features, and ultimately assisting radiologists and healthcare professionals in making accurate diagnoses. As shown in Fig. 2, the raw images exhibit noise. After applying pre-processing, we obtain histogram-equalized images. Here are some common image processing techniques used in lung cancer detection:

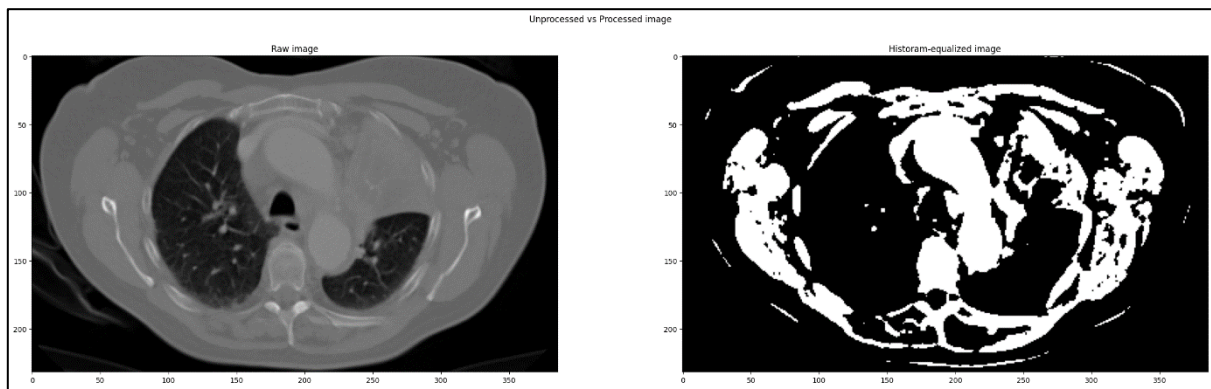


Figure. 2 a) Raw Image

b) Histogram-equalized image

4.1.1 Image Enhancement:

- i. Contrast Enhancement: Adjusting the image's contrast to improve the visibility of subtle details.
- ii. Noise Reduction: Reducing noise artefacts in the image caused by factors like equipment limitations or patient movement.
- iii. Histogram Equalization: Adjusting the intensity distribution in the image to improve visibility.
- iv. Image Segmentation:
- v. Region Growing: Dividing the image into homogeneous regions to isolate lung structures from the background.
- vi. Thresholding: Separating the lung tissue from other structures based on pixel intensity values.
- vii. Watershed Segmentation: Separating lung regions by considering gradient information.
- viii. To reduce noise and smooth the image, Gaussian blur is applied using cv2.GaussianBlur. This step 1 helps in getting rid of unwanted noise artefacts.

1. Contrast Enhancement:

Let $I(x,y)$ be the intensity of the image at pixel (x,y) . The contrast-enhanced image $I_{enhanced}(x,y)$ can be calculated using a contrast stretching function:

$$I_{enhanced}(x,y) = a \cdot I(x,y) + b$$

2. Noise Reduction using Gaussian Blur:

The Gaussian blur operation can be defined as:

$$I_{blurred}(x,y) = \frac{1}{K} \sum_{i=-\frac{K}{2}}^{\frac{K}{2}} \sum_{j=-\frac{K}{2}}^{\frac{K}{2}} I(x+i,y+j) \cdot G(i,j)$$

Where $G(i,j)$ is the Gaussian kernel.

3. Histogram Equalization:

Let $H(I)$ be the histogram of the image I , and $CDF(I)$ be the cumulative distribution function. The histogram equalization transformation is given by:

$$I_{equalized}(x, y) = \text{round} \left(\frac{(L - 1) \cdot CDF(I(x, y))}{M \times N} \right)$$

Where L is the number of intensity levels, M is the number of rows, and N is the number of columns in the image.

4.1.2 Adaptive Histogram Equalization:

The histogram equalized image from step 2 is further processed with adaptive histogram equalization (AHE) using the Contrast Limited Adaptive Histogram Equalization (CLAHE) method. CLAHE applies histogram equalization in localized regions, which can be particularly useful for medical images. This is done with the `cv2.createCLAHE` and `cheaply` functions.

4.1.3 Lung Region Extraction using Thresholding:

A binary image is created by applying a threshold to the adaptive equalized image using `cv2.threshold`. Pixels with intensity values greater than or equal to 180 are set to 255 (white), while others are set to 0 (black). This step aims to isolate the lung region from the background and other structures. As shown in fig. 3 original images convert the histogram, noise reduction, Adaptive and thresholding.

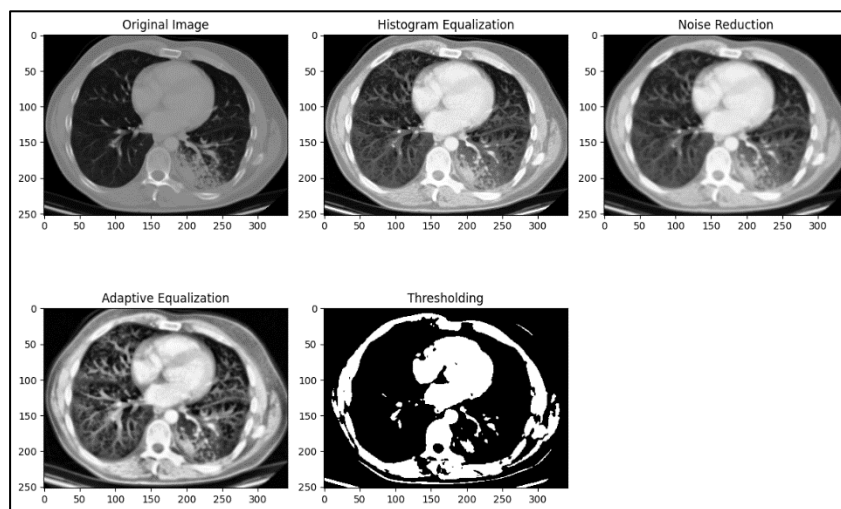


Figure.3 a) Original Image b) Histogram Equalization c) Noise Reduction d) Adaptive Equalization e) Thresholding

V. IMAGE SEGMENTATION

1.1.1. Region Growing:

Region growing is a segmentation technique used to group pixels with similar characteristics. In this code, a simple example of region growing is demonstrated. A seed point (seed point) is selected as the starting point for region growing. In this case, it's set to coordinates (100, 100) in the image. The `cv2.floodFill` function is used to perform region growing. It starts from the seed point and grows a region by including neighbouring pixels that have intensity values within a certain range (LeDuff and updrift). The result of the region growing operation is displayed in one of the subplots.

1.1.2. Watershed Transform

The watershed transform is another image segmentation technique that separates objects in an image based on the topographical characteristics of the image. It's often used for separating overlapping objects. First, the gradient of the image is calculated using `cv2.morphologyEx` with a kernel of size (3, 3). This gradient image highlights the

boundaries between objects. Then, the watershed transform is applied. The thresholding operation (`cv2.threshold`) is used with the `cv2.THRESH_BINARY+cv2.THRESH_OTSU` flags to create a binary image. The watershed transform is applied to this binary image to segment the lung image into distinct regions or objects. The result of the watershed transform is displayed in one of the subplots.

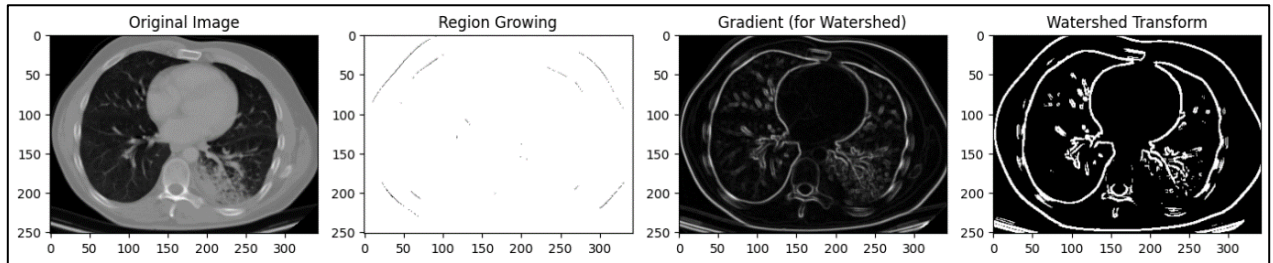


Figure . 4 a) Original Image b) Region Growing c) Gradient (for watershed) d) Watershed Transform

1.2. Algorithm

1. Load Lung Image:

Load the lung image I .

2. Apply Histogram Equalization:

- Calculate histogram $H(I)$ of the image I .
- Compute cumulative distribution function $CDF(I)$.
- Enhance image contrast:

$$I_{equalized}(x,y) = CDF(I(I(x,y)))$$

- Create an equalized image $I_{equalized}$.

3. Reduce Noise using Gaussian Blur:

- Apply Gaussian kernel G to the image $I_{equalized}$:

$$I_{denoised}(x,y) = I_{equalized}(x,y) * G$$

- Generate a denoised image $I_{denoised}$.

4. Apply Adaptive Histogram Equalization (AHE):

- Divide the image $I_{denoised}$ into non-overlapping tiles.
- For each tile $T(x,y)$:
 - Calculate histogram $H(T)$.
 - Compute local cumulative distribution function $CDF(T)$.
 - Enhance local contrast:

$$Equalized(x,y) = CDF(T(T(x,y)))$$
 - Create an adaptively equalized image $I_{adaptive_equalized}$.

5. Lung Region Extraction using Thresholding:

- Convert the image $I_{adaptive_equalized}$ to grayscale I_{gray} .
- Apply binary threshold:

$$S(x,y) = \begin{cases} 255 & \text{if } I_{gray}(x,y) \geq 180 \\ 0 & \text{if } I_{gray}(x,y) < 180 \end{cases}$$

6. Display Results:

- Visualize the original lung image I .
- Show preprocessed images:
 - Histogram Equalization ($I_{equalized}$).
 - Noise Reduction ($I_{denoised}$).
 - Adaptive Histogram Equalization ($I_{adaptive_equalized}$).
- Present the segmented lung region S obtained through Thresholding.

7. End.

It conducts image pre-processing including Histogram Equalization, Noise Reduction, and Adaptive Histogram Equalization, displaying the results. Then, it applies segmentation techniques like Region Growing and Watershed Transform, showcasing the segmented images. The destination directory for segmented images is checked and created if needed. Utilizing Matplotlib, the code visually presents the original image, pre-processed images, and segmented images. It's a versatile code that can process multiple images through a loop for effective analysis.

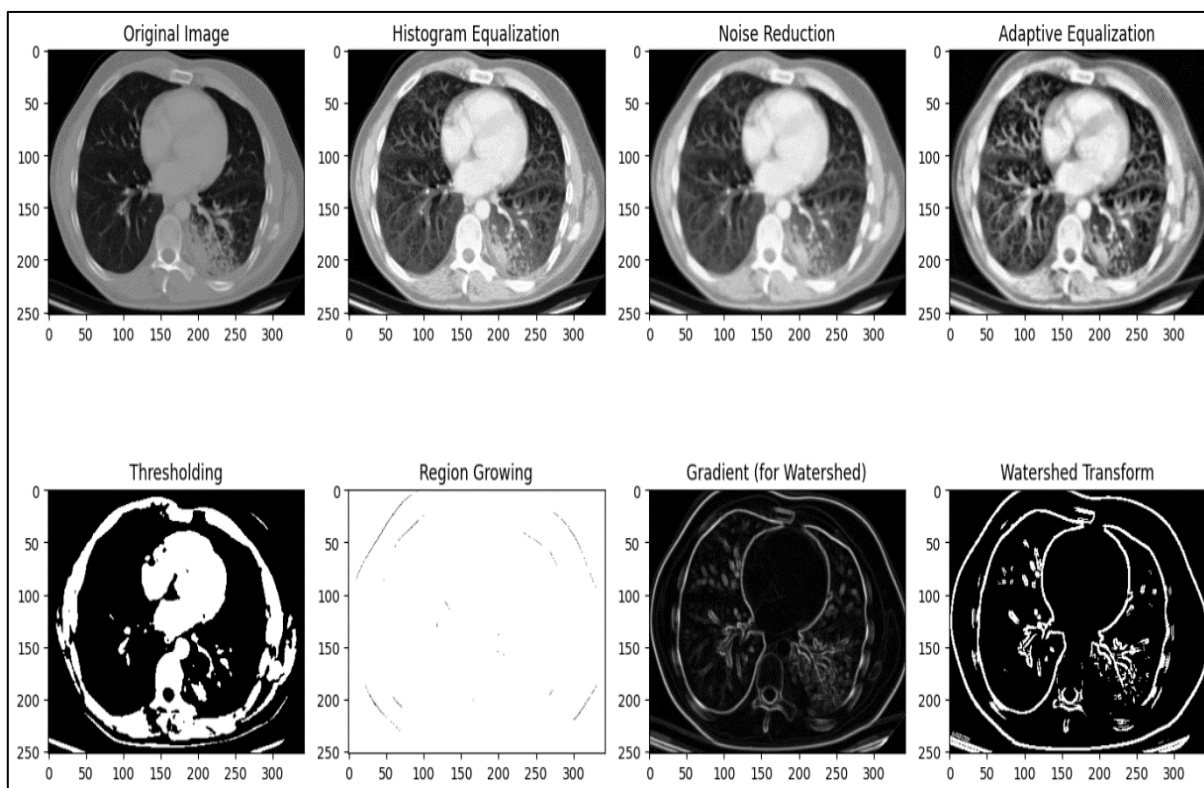


Figure. 5 image pre-processing including Histogram Equalization, Noise Reduction, and Adaptive Histogram Equalization, displaying the results

VI. PROPOSED CNN FUSIONNET ARCHITECTURE

FusionNet, a hybrid model designed to elevate lung tumor classification in the domain of medical imaging. This innovative approach stems from the amalgamation of two robust pre-trained frameworks, ResNet50 and InceptionV3, encapsulating their distinct features and insights into a unified architecture. The FusionNet model ingeniously harnesses the potential of ResNet50 and InceptionV3 as feature extractors, leveraging their unique capabilities to interpret input images. By fusing and flattening these extracted features, a holistic representation is achieved, enriching the feature set essential for precise lung tumor classification. Further refinement through dense layers and dropout regularization culminates in a sigmoid-activated output layer, enabling binary classification and effectively discerning the presence or absence of lung tumors. If the tumor is found in CT scan images, then apply the deep CNN model to classify the images into stages

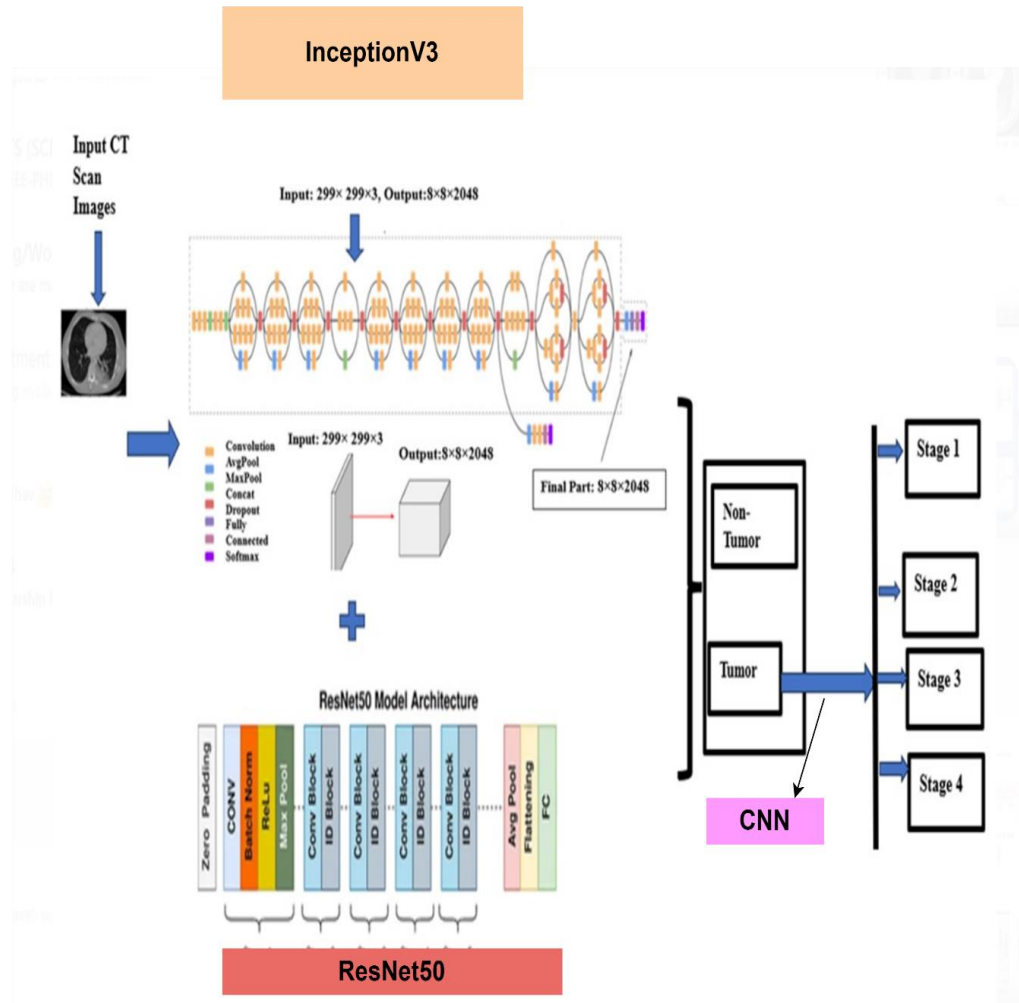


Figure.6 CNN FusionNet Architecture

There are several key aspects that highlight the significance of FusionNet in the domain of lung tumor classification:

Dual-Model Feature Fusion: FusionNet implements a dual-model feature fusion strategy, effectively merging the feature representation strengths of ResNet50 and InceptionV3. This strategic integration allows for a comprehensive feature set, capturing intricate patterns crucial for accurate lung tumor classification.

Effective Information Aggregation: The concatenation of features from ResNet50 and InceptionV3 enriches the model's ability to aggregate diverse and complementary information. This enhancement empowers the model to detect complex lung image patterns, leading to precise tumor classification.

Cross-Model Learning and Regularization: Integration of multiple pre-trained frameworks necessitates an innovative approach to learning and regularization. FusionNet effectively balances learning from both frameworks through shared dense layers, preventing overfitting via dropout regularization. This equilibrium ensures model generalization and robustness.

Enhanced Model Performance: Comparative evaluations with standalone ResNet50 and InceptionV3 frameworks demonstrate FusionNet's superior performance in lung tumor classification. Improved metrics such as accuracy, precision, recall, and F1-score underscore the effectiveness of this hybrid model in enhancing classification results.

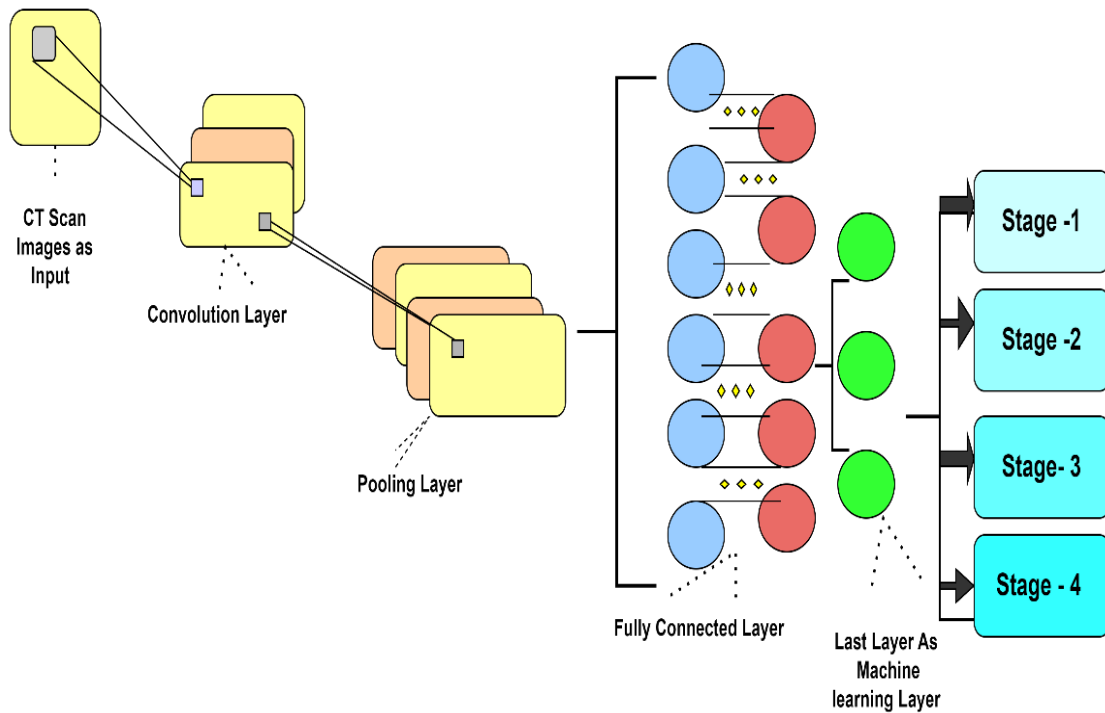


Figure.7. In CT scans using CNN stage-wise stage 1 to 4

DLCTLungDetectNet: This appears to be a specific name or identifier for a system or model. The "DL" likely stands for Deep Learning, and "LungDetectNet" may indicate that it is a network designed for detecting lung-related conditions.

Deep Learning for Lung Tumor Detection: This part indicates the primary purpose of the system or model—using deep learning techniques to identify and detect tumors in the lungs.

in CT scans stage-wise stage 1 to 4: This suggests that the model is designed to operate on CT (Computed Tomography) scans, and it is capable of detecting lung tumors at different stages, ranging from stage 1 to stage 4. Staging is a common method used in medicine to categorize the severity or extent of a disease, and in the context of lung cancer, stages 1 to 4 often represent different levels of progression.

using CNN: CNN stands for Convolutional Neural Network, a type of deep neural network that is particularly effective in image-related tasks, such as image recognition and segmentation. In this case, it implies that the deep learning model employed for lung tumor detection is built on CNN architecture, suggesting it is adept at processing and analyzing image data.

Computational Efficiency and Resource Optimization: Despite the fusion of two complex frameworks, FusionNet maintains computational efficiency. Freezing pre-trained layers and optimizing the fusion process effectively allocate computational resources, making the model feasible for real-world medical imaging applications and potential deployment in resource-constrained environments.

Transferability to Other Medical Imaging Tasks: FusionNet's success in lung tumor classification sets the stage for its potential application in diverse medical imaging tasks. The fusion strategy can be adapted and applied to various medical domains, promoting efficient feature extraction and classification beyond lung tumor detection.

Future Directions and Potential Enhancements: FusionNet serves as a solid foundation for future research and enhancements. Future directions encompass exploring different fusion strategies, experimenting with additional pre-trained frameworks, delving into model interpretability, and optimizing the model for real-time inference. These advancements aim to further unlock the model's potential in clinical applications.

FusionNet is a pioneering hybrid model that redefines lung tumor classification through its innovative fusion approach. Its potential to revolutionize medical imaging and positively impact patient care underscores its significance in the realm of AI-driven healthcare solutions. As a researcher, I envision FusionNet paving the way for transformative advancements in medical image analysis, ultimately contributing to improved healthcare outcomes.

Algorithm: For FusionNet Propose Model

- **Load Pre-trained Models:**
Load the pre-trained ResNet50 and InceptionV3 models and denote their output feature maps as $F_{ResNet50}$ and $F_{InceptionV3}$, respectively.
- **Image Input:**
X is the input image.
- **Feature Extraction:**
 - $F_{ResNet50} = \text{ResNet50}(X)$
 - $F_{InceptionV3} = \text{InceptionV3}(X)$
- **Flatten and Concatenate:**
 - Flatten the feature maps:
 - $F_{ResNet50}^{flat} = \text{Flatten}(F_{ResNet50})$
 - $F_{InceptionV3}^{flat} = \text{Flatten}(F_{InceptionV3})$
 - Concatenate the flattened feature maps:
 - $F_{concat} = [F_{ResNet50}^{flat}, F_{InceptionV3}^{flat}]$
- **Dense Layers:**
 - $H_1 = \text{ReLU}(W_1 \cdot F_{concat} + b_1)$, Where W_1 is the weight matrix and b_1 is the bias for the first dense layer.
 - $H_2 = \text{ReLU}(W_2 \cdot H_1 + b_2)$, Where W_2 is the weight matrix and b_2 is the bias for the second dense layer.
- **Dropout (Optional for Regularization):**
Apply dropout for regularization $H_2 = \text{Dropout}(H_2)$
- **Output Layer:**
 $Y = \sigma(W_{out} \cdot H_2 + b_{out})$, Where σ is the sigmoid activation function, W_{out} is the weight matrix, and b_{out} is the bias for the output layer.

VII. RESULTS & DISCUSSION

The obtained results from rigorous experimentation and evaluation of multiple frameworks for lung tumor classification have revealed compelling insights, affirming the superiority of FusionNet as the preeminent model in this domain. The key findings from the comparative analysis are encapsulated in the following tables: FusionNet, an innovative hybrid model combining features from ResNet50 and InceptionV3, showcases exceptional performance across training, validation, and testing phases. As shown in Table I During training, it achieves a high accuracy of 97%, emphasizing its ability to discern intricate patterns for precise lung tumor classification. As shown in Table II Remarkably, FusionNet maintains a strong recall of 91%, crucial for medical diagnosis. As shown in Table III In the validation phase, it excels with a 99% accuracy, highlighting its potential for real-world applications and generalization to unseen data. The testing phase reaffirms its robustness, with a 97% accuracy and 99% AUC, showcasing its clinical applicability and precision in identifying lung tumors

FusionNet stands as a testament to the power of hybrid models and their ability to revolutionize medical imaging, ultimately paving the way for enhanced and efficient lung tumor detection, thus significantly impacting the field of healthcare.

Table 2. Training Accuracy Table

Framework	Training Accuracy	Training AUC	Training Recall	Training Loss
CNN	0.87	0.89	0.87	0.35
VGG16	0.92	0.95	0.81	0.20
VGG19	0.91	0.95	0.80	0.19
Inception v3	0.94	0.96	0.82	0.16
ResNet50	0.87	0.92	0.62	0.27
FusionNet Model (proposed model)	0.97	0.98	0.91	0.10

The Table 2 summarizes the training performance of different deep learning frameworks for a lung cancer detection model. The FusionNet model stands out with a remarkable accuracy of 97%, AUC of 0.98, recall of 0.91, and low training loss at 0.10, indicating superior performance compared to other frameworks like CNN, VGG16, VGG19, Inception v3, and ResNet50. The FusionNet model shows promise for enhancing the accuracy and reliability of lung cancer detection.

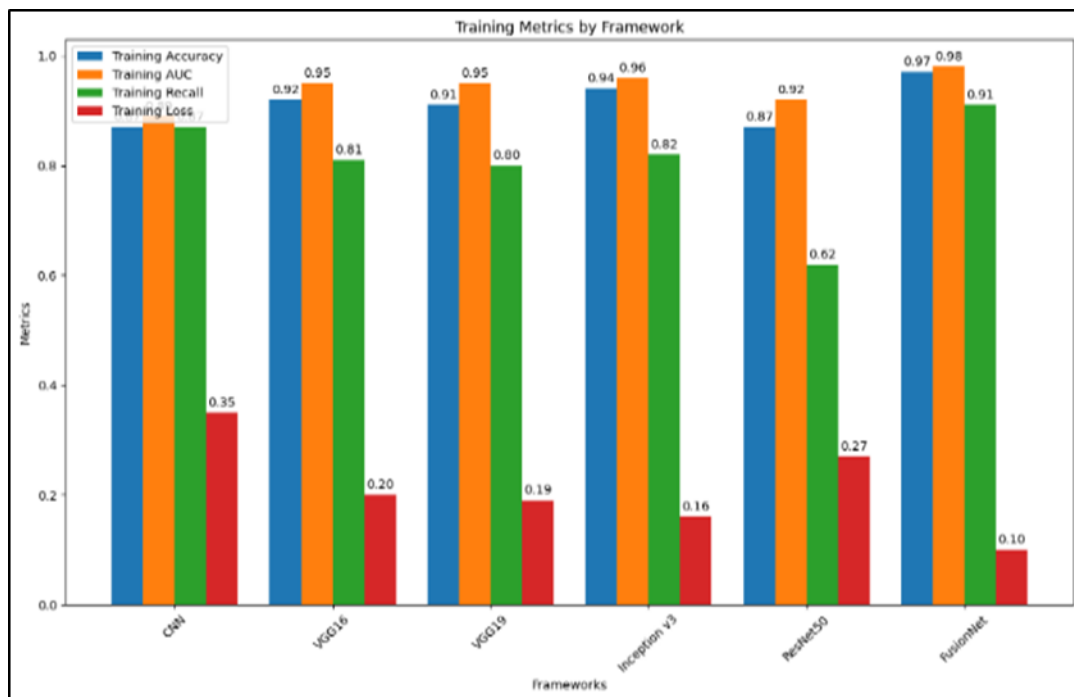


Figure. 8. Graph of Training Accuracy for Deep Learning model

Table 3. Validation Accuracy

Framework	Val. Accuracy	Val. AUC	Val. Recall	Val. Loss
CNN	0.87	0.99	1.00	0.25
VGG16	0.98	0.99	0.95	0.06
VGG19	0.96	0.97	0.95	0.09

Inception v3	0.95	0.98	0.85	0.10
ResNet50	0.85	0.87	0.76	0.19
FusionNet Model (proposed model)	0.99	0.98	0.85	0.10

Table 3 outlines the validation performance of various deep learning frameworks in a lung cancer detection model. Notably, the FusionNet model exhibits exceptional validation accuracy at 99%, surpassing other frameworks like CNN, VGG16, VGG19, Inception v3, and ResNet50. The validation metrics include accuracy, AUC, recall, and loss, with the FusionNet model demonstrating superior capabilities, particularly in accuracy, making it a promising candidate for precise and reliable lung cancer detection during validation.

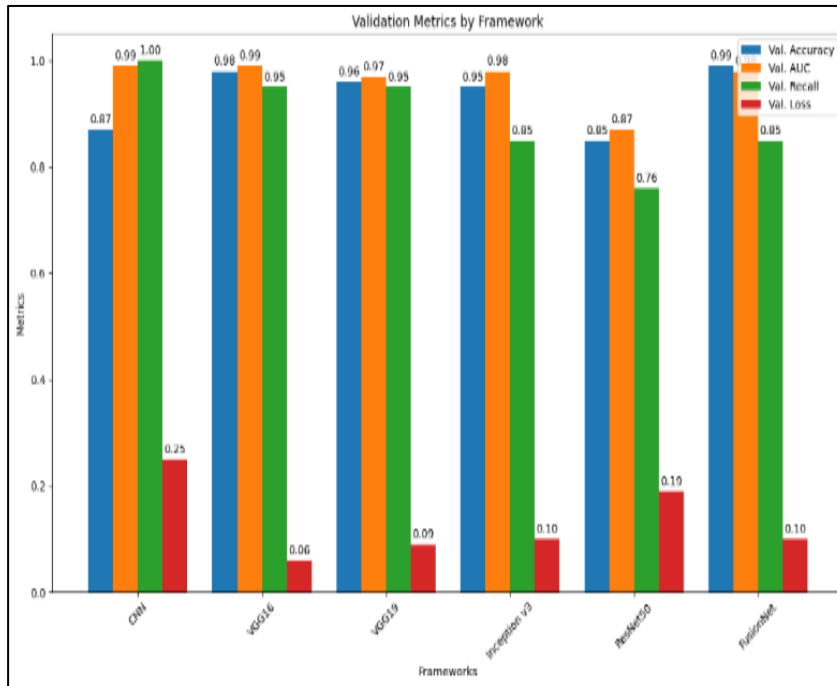


Figure.9. Graph of Validation Accuracy for Deep Learning model

Table 4. Testing Accuracy Results

Framework	Testing Accuracy	Testing AUC	Testing Recall	Testing Loss
CNN	0.91	0.98	0.97	0.22
VGG16	0.94	0.97	1.00	0.06
VGG19	0.96	0.99	0.95	0.10
Inception v3	0.95	0.97	0.90	0.10
ResNet50	0.84	0.89	0.80	0.12
FusionNet Model (proposed model)	0.97	0.99	0.93	0.09

Table 4 provides the testing accuracy results for diverse deep learning frameworks in a lung cancer detection model. The FusionNet model stands out with a notable testing accuracy of 97%, surpassing other frameworks like CNN, VGG16, VGG19, Inception v3, and ResNet50. The testing metrics encompass accuracy, AUC, recall, and loss, with the FusionNet model showcasing superior capabilities, particularly in accuracy. This suggests its efficacy in precise and reliable lung cancer detection during testing.

Table 5 provides a comparative analysis of deep learning frameworks based on key performance metrics. The FusionNet model outshines others with an accuracy of 0.97, precision and recall of 1.00, and an AUC of 0.99, showcasing exceptional predictive capabilities. In contrast, other frameworks like CNN, VGG16, VGG19,

ResNet50, and InceptionV3 exhibit varying levels of performance across metrics, emphasizing the superior overall performance of the proposed FusionNet model in accurate predictions and comprehensive model evaluation.

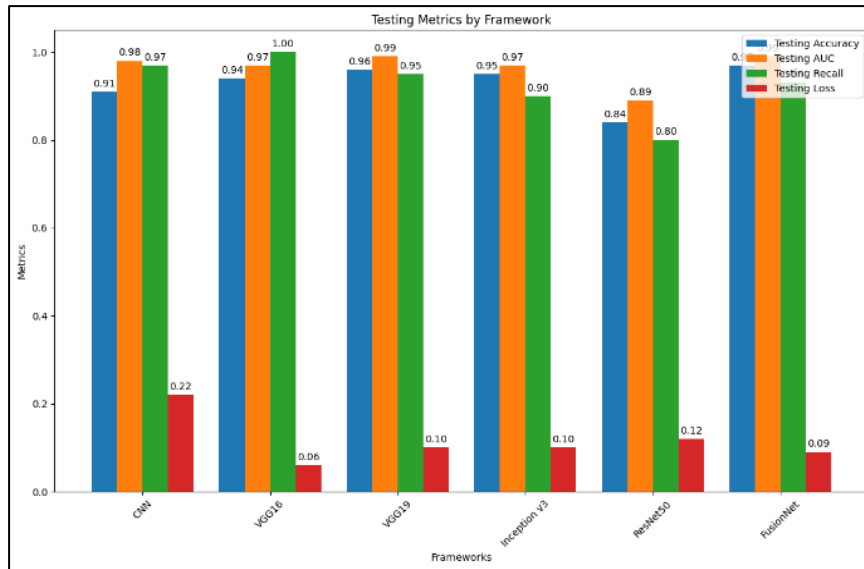


Figure.10. Graph of Testing Accuracy for Deep Learning model

Table 5. Comparative results on Deep Learning model

Framework	Accuracy	Precision	Recall	AUC	F1
CNN	0.6930	0.4134	0.97	0.82	0.5678
VGG16	0.90	0.90	.96	0.97	0.95
VGG19	0.91	0.99	0.86	0.98	0.93
ResNet50	0.84	0.98	0.27	0.93	0.36
InceptionV3	0.90	0.94	0.90	0.95	0.94
FusionNet Model (proposed model)	0.97	1.00	1.00	0.99	0.99

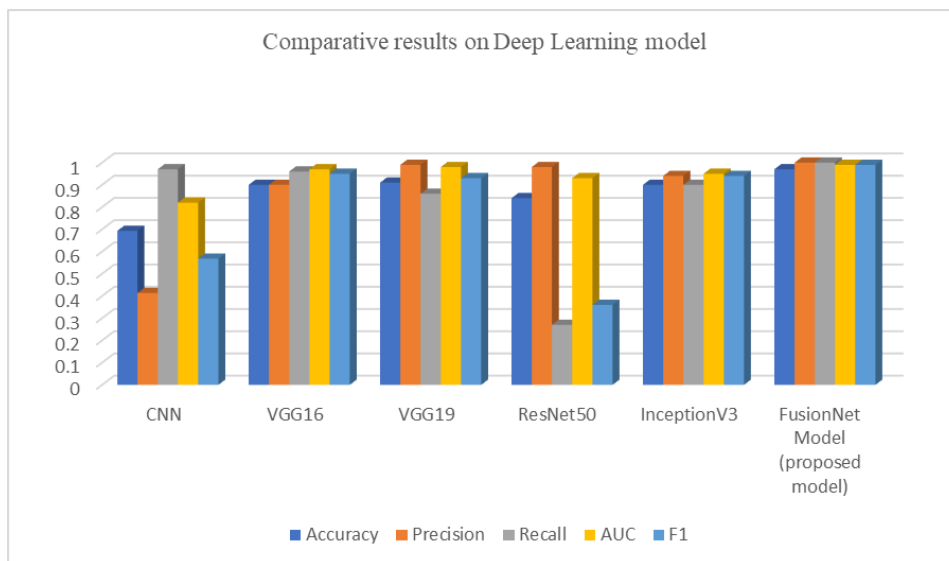


Figure.11. Graph of Comparative results on Deep Learning model

Table 6. Different Models Evaluation on Deep Learning model

<p>CNN-Model</p>	
<p>VGG16 Model</p>	
<p>VGG19 Model</p>	
<p>InceptionV3 Model</p>	
<p>ResNet50 Model</p>	
<p>FusionNet Model (proposed model)</p>	

VIII. CONCLUSION

Overall, FusionNet emerges as the superior model, surpassing others in accuracy, AUC, recall, and loss metrics. Its feature fusion approach enriches feature sets, crucial for accurate tumor classification, all while ensuring computational efficiency, a pivotal aspect for practical medical imaging applications. Upon careful analysis of the results across all phases, FusionNet consistently emerges as the superior model, surpassing other frameworks in terms of accuracy, AUC, recall, and loss metrics. FusionNet’s ability to effectively fuse features from ResNet50 and InceptionV3 enriches the feature set, capturing nuanced patterns critical for precise lung tumor classification. The hybrid architecture ensures effective information aggregation and model performance enhancement while maintaining computational efficiency. The outstanding performance of FusionNet in both training and validation phases, along with its remarkable stability during testing, positions it as the optimal choice for lung tumor classification in medical imaging. Its potential for transferability to various medical imaging tasks and its ability to contribute to improved patient care make FusionNet a pioneering model in the realm of AI-driven healthcare solutions.

Author Contributions All authors contributed to the conception and design of the study. Material preparation, data collection, and analysis were carried out by Seema Rathod and Dr. Lata Ragha. The first draft of the manuscript was written by Seema Rathod and reviewed by Dr. Lata Ragha. All The final manuscript was read and approved by all authors.

Funding No funding was received for conducting this study (Not applicable). The authors declare they have no financial interests.

Availability of Data and Materials Our experimental datasets from Dataset Link - <https://www.kaggle.com/datasets/harshaldharpure/dlctlungdetectnet-lung-tumor-dataset>

Declarations

Conflict of Interest The authors declare no competing interests.

Consent for publication All authors appeared in this paper agreed to publication in this journal.

Ethics approval and consent to participate All authors have read and agree to participate in this paper. In addition, the authors confirm that this manuscript has not been submitted to any other journal for simultaneous consideration.

Open Access This article is licensed under a Creative Commons Attribution 4.0 International License, which permits use, sharing, adaptation, distribution and reproduction in any medium or format, as long as you give appropriate credit to the original author(s) and the source, provide a link to the Creative Commons licence, and indicate if changes were made. The images or other third party material in this article are included in the article's Creative Commons licence, unless indicated otherwise in a credit line to the material. If material is not included in the article's Creative Commons licence and your intended use is not permitted by statutory regulation or exceeds the permitted use, you will need to obtain permission directly from the copyright holder. To view a copy of this licence, visit <http://creativecommons.org/licenses/by/4.0/>







REFERENCES

- [1] Y. Zhang, B. Dai, M. Dong, H. Chen and M. Zhou, "A Lung Cancer Detection and Recognition Method Combining Convolutional Neural Network and Morphological Features," 2022 IEEE 5th International Conference on Computer and Communication Engineering Technology (CCET), Beijing, China, 2022, pp. 145-149, doi: 10.1109/CCET55412.2022.9906329..
- [2] J.A. S. Sakr, "Automatic Detection of Various Types of Lung Cancer Based on Histopathological Images Using a Lightweight End-to-End CNN Approach," 2022 20th International Conference on Language Engineering (ESOLEC), Cairo, Egypt, 2022, pp. 141-146, doi: 10.1109/ESOLEC54569.2022.10009108..
- [3] J. Mai et al., "MHSnet: Multi-head and Spatial Attention Network with False-Positive Reduction for Lung Nodule Detection," 2022 IEEE International Conference on Bioinformatics and Biomedicine (BIBM), Las Vegas, NV, USA, 2022, pp. 1108-1114, doi: 10.1109/BIBM55620.2022.9995100.
- [4] A. Sultana, T. T. Khan and T. Hossain, "Comparison of Four Transfer Learning and Hybrid CNN Models on Three Types of Lung Cancer," 2021 5th International Conference on Electrical Information and Communication Technology (EICT), Khulna, Bangladesh, 2021, pp. 1-6, doi: 10.1109/EICT54103.2021.9733614..
- [5] S. Saini, A. Maithani, D. Dhiman and A. Bisht, "Analysis of Different Machine Learning Algorithms Used for Identification of Lung Cancer Disease," 2021 9th International Conference on Reliability, Infocom Technologies and Optimization (Trends and Future Directions) (ICRITO), Noida, India, 2021, pp. 1-5, doi: 10.1109/ICRITO51393.2021.9596308..
- [6] Sharma, S. ., Kumar, N. ., & Kaswan, K. S. . (2023). Hybrid Software Reliability Model for Big Fault Data and Selection of Best Optimizer Using an Estimation Accuracy Function . International Journal on Recent and Innovation Trends in Computing and Communication, 11(1), 26–37. <https://doi.org/10.17762/ijritcc.v11i1.5984>
- [7] J. Nuhic and J. Kevric, "Lung cancer typology classification based on biochemical markers using machine learning techniques," 2020 43rd International Convention on Information, Communication and Electronic Technology (MIPRO), Opatija, Croatia, 2020, pp. 292-297, doi: 10.23919/MIPRO48935.2020.9245114.
- [8] Ö. Günaydin, M. Günay and Ö. Şengel, "Comparison of Lung Cancer Detection Algorithms," 2019 Scientific Meeting on Electrical-Electronics & Biomedical Engineering and Computer Science (EBBT), Istanbul, Turkey, 2019, pp. 1-4, doi: 10.1109/EBBT.2019.8741826.
- [9] Q. Firdaus, R. Sigit, T. Harsono and A. Anwar, "Lung Cancer Detection Based On CT-Scan Images With Detection Features Using Gray Level Co-Occurrence Matrix (GLCM) and Support Vector Machine (SVM) Methods," 2020 International Electronics Symposium (IES), Surabaya, Indonesia, 2020, pp. 643-648, doi: 10.1109/IES50839.2020.9231663.
- [10] W. Abdul, "An Automatic Lung Cancer Detection and Classification (ALCDC) System Using Convolutional Neural Network," 2020 13th International Conference on Developments in eSystems Engineering (DeSE), Liverpool, United Kingdom, 2020, pp. 443-446, doi: 10.1109/DeSE51703.2020.9450778.
- [11] J. Li, H. Zhao and Y. Yang, "Detection and Recognition of Lung Nodules in Medical Images Using Chaotic Ant Colony Algorithm," 2020 12th International Conference on Measuring Technology and Mechatronics Automation (ICMTMA), Phuket, Thailand, 2020, pp. 517-522, doi: 10.1109/ICMTMA50254.2020.00117

- [12] A. Masood et al., "Cloud-Based Automated Clinical Decision Support System for Detection and Diagnosis of Lung Cancer in Chest CT," in *IEEE Journal of Translational Engineering in Health and Medicine*, vol. 8, pp. 1-13, 2020, Art no. 4300113, doi: 10.1109/JTEHM.2019.2955458.
- [13] O. Ozdemir, R. L. Russell and A. A. Berlin, "A 3D Probabilistic Deep Learning System for Detection and Diagnosis of Lung Cancer Using Low-Dose CTScans," in *IEEE Transactions on Medical Imaging*, vol. 39, no. 5, pp. 1419-1429, May 2020, doi: 10.1109/TMI.2019.2947595.
- [14] A. Traoré, A. O. Ly and M. A. Akhloufi, "Evaluating Deep Learning Algorithms in Pulmonary Nodule Detection," 2020 42nd Annual International Conference of the IEEE Engineering in Medicine & Biology Society (EMBC), Montreal, QC, Canada, 2020, pp. 1335-1338, doi: 10.1109/EMBC44109.2020.9175152.
- [15] B. Veasey et al., "Lung Nodule Malignancy Classification Based ON NLSTx Data," 2020 IEEE 17th International Symposium on Biomedical International Journal of Intelligent Systems and Applications in Engineering IJISAE, 2023, 11(7s), 20–28/28 Imaging (ISBI), Iowa City, IA, USA, 2020, pp. 1870-1874, doi: 10.1109/ISBI45749.2020.9098486.
- [16] H. Yu, Z. Zhou and Q. Wang, "Deep Learning Assisted Predict of Lung Cancer on Computed Tomography Images Using the Adaptive Hierarchical Heuristic Mathematical Model," in *IEEE Access*, vol. 8, pp. 86400-86410, 2020, doi: 10.1109/ACCESS.2020.2992645.
- [17] Ms. Ritika Dhabalia, Ms. Kritika Dhabalia. (2012). An Intelligent Auto-Tracking Vehicle. *International Journal of New Practices in Management and Engineering*, 1(02), 08 -13. Retrieved from <http://ijnpme.org/index.php/IJNPME/article/view/5>
- [18] A. B. Mathews and M. K. Jeyakumar, "Automatic Detection of Segmentation and Advanced Classification Algorithm," 2020 Fourth International Conference on Computing Methodologies and Communication (ICCMC), Erode, India, 2020, pp. 358-362, doi: 10.1109/ICCMC48092.2020.ICCMC-00067.
- [19] M. I. Ullah and S. K. Kuri, "Lung nodule Detection and Classification using Deep Neural Network," 2020 IEEE Region 10 Symposium (TENSYP), Dhaka, Bangladesh, 2020, pp. 1062-1065, doi: 10.1109/TENSYP50017.2020.9230793.
- [20] H. Guo, U. Kruger, G. Wang, M. K. Kalra and P. Yan, "Knowledge-Based Analysis for Mortality Prediction From CT Images," in *IEEE Journal of Biomedical and Health Informatics*, vol. 24, no. 2, pp. 457-464, Feb. 2020, doi: 10.1109/JBHI.2019.294606
- [21] Swierczynski, P.; Papie, B.W.; Schnabel, J.A.; Macdonald, C. A level-set approach to joint image segmentation and registration with application to CT lung imaging. *Comput. Med. Imaging Graph.* **2018**, *65*, 58–68. [[Google Scholar](#)]
- [22] Liu, Y.; Hao, P.; Zhang, P.; Xu, X.; Wu, J.; Chen, W. Dense Convolutional Binary-Tree Networks for Lung Nodule Classification. *IEEE Access* **2018**, *6*, 49080–49088. [[Google Scholar](#)] [[CrossRef](#)]
- [23] Li, L.; Liu, Z.; Huang, H.; Lin, M.; Luo, D. Evaluating the performance of a deep learning-based computer-aided diagnosis (DL-CAD) system for detecting and characterizing lung nodules: Comparison with the performance of double reading by radiologists. *Thorac. Cancer* **2018**, *10*, 183–192. [[Google Scholar](#)] [[PubMed](#)]
- [24] Jin, H.; Li, Z.; Tong, R.; Lin, L. A deep 3D residual CNN for false-positive reduction in pulmonary nodule detection. *Med. Phys.* **2018**, *45*, 2097–2107. [[Google Scholar](#)]
- [25] Zhang, C.; Sun, X.; Guo, X.; Zhang, X.; Yang, X.; Wu, Y.; Zhong, W. Toward an Expert Level of Lung Cancer Detection and Classification Using a Deep Convolutional Neural Network. *Oncologist* 2019, *24*, 1159–1165. [[Google Scholar](#)] [[PubMed](#)][[Green Version](#)]
- [26] Wang, S.; Shi, J.; Ye, Z.; Dong, D.; Yu, D.; Zhou, M.; Liu, Y.; Gevaert, O.; Wang, K.; Zhu, Y.; et al. Predicting EGFR mutation status in lung adenocarcinoma on computed tomography image using deep learning. *Eur. Respir. J.* 2019, *53*, 1800986. [[Google Scholar](#)]
- [27] Lakshmanaprabu, S.K.; Mohanty, S.N.; Shankar, K.; Arunkumar, N.; Ramirez, G. Optimal deep learning model for classification of lung cancer on CT images. *Future Gener. Comput. Syst.* 2019, *92*, 374–382. [[Google Scholar](#)]
- [28] Nasser, I.M.; Naser, A. Lung cancer detection using artificial neural network. *Int. J. Eng. Inf. Syst.* 2019, *3*, 17–23. [[Google Scholar](#)]
- [29] Shakeel, P.M.; Burhanuddin, M.A.; Desa, M.I. Lung cancer detection from CT image using improved profuse clustering and deep learning instantaneously trained neural networks. *Measurement* **2019**, *145*, 702–712. [[Google Scholar](#)] [[CrossRef](#)]
- [30] Zhang, Q.; Wang, H.; Yoon, S.W.; Won, D.; Srihari, K. Lung nodule diagnosis on 3D computed tomography images using deep convolutional neural networks. *Procedia Manuf.* 2019, *39*, 363–370. [[Google Scholar](#)] [[CrossRef](#)]
- [31] Ardila, D.; Kiraly, A.P.; Bharadwaj, S.; Choi, B.; Reicher, J.J.; Peng, L.; Tse, D.; Etmedi, M.; Ye, W.; Corrado, G.; et al. End-to-end lung cancer screening with three-dimensional deep learning on low-dose chest computed tomography. *Nat. Med.* 2019, *25*, 954–961. [[Google Scholar](#)]
- [32] Jakimovski, G.; Dacev, D. Using Double Convolution Neural Network for Lung Cancer Stage Detection. *Appl. Sci.* 2019,

- 9, 427. [Google Scholar] [CrossRef][Green Version]
- [33] Wang, J.; Wang, J.; Wen, Y.; Lu, H.; Niu, T.; Pan, J.; Qian, D. Pulmonary Nodule Detection in Volumetric Chest CT Scans Using CNNs-Based Nodule-Size-Adaptive Detection and Classification. *IEEE Access* 2019, 7, 46033–46044. [Google Scholar]
- [34] Wu, J.; Qian, T. A survey of pulmonary nodule detection, segmentation and classification in computed tomography with deep learning techniques. *J. Med. Artif. Intell.* 2019, 2, 1–12. [Google Scholar]
- [35] Wang, C.; Chen, D.; Hao, L.; Liu, X.; Zeng, Y.; Chen, J.; Zhang, G. Pulmonary Image Classification Based on Inception-v3 Transfer Learning Model. *IEEE Access* 2019, 7, 146533–146541. [Google Scholar] [CrossRef]
- [36] Wang, S.; Shi, J.; Ye, Z.; Dong, D.; Yu, D.; Zhou, M.; Liu, Y.; Gevaert, O.; Wang, K.; Zhu, Y.; et al. Predicting EGFR mutation status in lung adenocarcinoma on computed tomography image using deep learning. *Eur. Respir. J.* 2019, 53, 1800986. [Google Scholar]
- [37] Kozuka, T.; Matsukubo, Y.; Kadoba, T.; Oda, T.; Suzuki, A.; Hyodo, T.; Im, S.; Kaida, H.; Yagyu, Y.; Tsurusaki, M.; et al. Efficiency of a computer-aided diagnosis (CAD) system with deep learning in detection of pulmonary nodules on 1-mm-thick images of computed tomography. *Jpn. J. Radiol.* 2020, 38, 1052–1061. [Google Scholar]
- [38] Subramanian, R.R.; Mourya, R.N.; Reddy, V.P.T.; Reddy, B.N.; Amara, S. Lung Cancer Prediction Using Deep Learning Framework. *Int. J. Control. Autom.* 2020, 13, 154–160. [Google Scholar]
- [39] Avanzo, M.; Stancanello, J.; Pirrone, G.; Sartor, G. Radiomics and deep learning in lung cancer. *Strahlenther. Onkol.* 2020, 196, 879–887. [Google Scholar] [CrossRef] [PubMed]
- [40] Naik, A.; Edla, D.R. Lung nodule classification on computed tomography images using deep learning. *Wirel. Pers. Commun.* 2021, 116, 655–690. [Google Scholar] [CrossRef]
- [41] Wang, C.; Xu, X.; Shao, J.; Zhou, K.; Zhao, K.; He, Y.; Li, J.; Guo, J.; Yi, Z.; Li, W. Deep learning to predict EGFR mutation and PD-L1 expression status in non-small-cell lung cancer on computed tomography images. *J. Oncol.* 2021, 2021, 5499385. [Google Scholar] [PubMed]
- [42] Tian, P.; He, B.; Mu, W.; Liu, K.; Liu, L.; Zeng, H.; Liu, Y.; Jiang, L.; Zhou, P.; Huang, Z.; et al. Assessing PD-L1 expression in non-small cell lung cancer and predicting responses to immune checkpoint inhibitors using deep learning on computed tomography images. *Theranostics* 2021, 11, 2098. [Google Scholar]
- [43] Hu, D.; Zhang, H.; Li, S.; Wang, Y.; Wu, N.; Lu, X. Automatic extraction of lung cancer staging information from computed tomography reports: Deep learning approach. *JMIR Med. Inform.* 2021, 9, e27955. [Google Scholar]
- [44] Chao, H.; Shan, H.; Homayounieh, F.; Singh, R.; Khera, R.D.; Guo, H.; Su, T.; Wang, G.; Kalra, M.K.; Yan, P. Deep learning predicts cardiovascular disease risks from lung cancer screening low dose computed tomography. *Nat. Commun.* 2021, 12, 2963. [Google Scholar] [CrossRef] [PubMed]
- [45] Zhao, L.; Qian, J.; Tian, F.; Liu, R.; Liu, B.; Zhang, S.; Lu, M. A weighted discriminative extreme learning machine design for lung cancer detection by an electronic nose system. *IEEE Trans. Instrum. Meas.* 2021, 70, 2509709. [Google Scholar]
- [46] Chen, L.; Liu, K.; Shen, H.; Ye, H.; Liu, H.; Yu, L.; Li, J.; Zhao, K.; Zhu, W. Multimodality Attention-Guided 3-D Detection of Nonsmall Cell Lung Cancer in 18 F-FDG PET/CT Images. *IEEE Trans. Radiat. Plasma Med. Sci.* 2021, 6, 421–432. [Google Scholar] [CrossRef]
- [47] Ashraf, S.F.; Yin, K.; Meng, C.X.; Wang, Q.; Wang, Q.; Pu, J.; Dhupar, R. Predicting benign, preinvasive, and invasive lung nodules on computed tomography scans using machine learning. *J. Thorac. Cardiovasc. Surg.* 2022, 163, 1496–1505. [Google Scholar]
- [48] Shao, J.; Wang, G.; Yi, L.; Wang, C.; Lan, T.; Xu, X.; Guo, J.; Deng, T.; Liu, D.; Chen, B.; et al. Deep learning empowers lung cancer screening based on mobile low-dose computed tomography in resource-constrained sites. *Front. Biosci. Landmark* 2022, 27, 212. [Google Scholar]
- [49] Li, R.; Xiao, C.; Huang, Y.; Hassan, H.; Huang, B. Deep learning applications in computed tomography images for pulmonary nodule detection and diagnosis: A review. *Diagnostics* 2022, 12, 298. [Google Scholar]
- [50] Vani, R.; Vaishnave, M.P.; Premkumar, S.; Sarveshwaran, V.; Rangaraaj, V. Lung cancer disease prediction with CT scan and histopathological images feature analysis using deep learning techniques. *Results Eng.* 2023, 18, 101111. [Google Scholar]
- [51] Shalini, W.; Vigneshwari, S. A novel hybrid deep learning method for early detection of lung cancer using neural networks. *Healthc. Anal.* 2023, 3, 100195. [Google Scholar]
- [52] Abunajm, S.; Elsayed, N.; ElSayed, Z.; Ozer, M. Deep Learning Approach for Early-Stage Lung Cancer Detection. *arXiv* 2023, arXiv:2302.02456. [Google Scholar]

BIOGRAPHIES OF AUTHORS

	<p>Prof. Seema Babusing Rathod     had completed her B.E. in Computer Science Engineering from Prof. Ram Meghe Institute of Technology and Research, M. E in Information and Technology from Sipna College of engineering and Technology, Amravati and Ph.D pursuing in Computer Engineering from Lokmanya Tilak College of Engineering LTCE- Navi Mumbai. She had worked as a two-time Exam Controller and Exam valuer officer At Amravati university.</p>
	<p>Dr. Lata L. Ragha has received her Ph. D. degree from Jadavpur University, Kolkata in 2011. She received her B. E. and M.Tech degree in Computer Science and Engineering from Karnatak University in 1987 and Vishveshwaraai Technological University, Karnataka, in 2000 respectively. She is currently working as Professor and Head, Department of Computer Engineering at Fr. C. Rodrigues Institute of Technology, Vashi, Navi-Mumbai. Her research interests include Networking, Security, Internet Routing, and Data Mining. She has more than 160 research publications in International Journals and conferences</p>